HYDROELASTIC PHENOMENA IN BOILING WATER REACTOR SUPPRESSION POOLS

B. D. NICHOLS, C. W. HIRT

Theoretical Division, Group T-3, University of California, Los Alamos Scientific Laboratory, P.O. Box 1663, Los Alamos, New Mexico 87545, U.S.A.

SUMMARY

In a postulated loss-of-coolant accident (LOCA) in a boiling water reactor (BWR) air is initially forced through vents into large water pools designed for steam pressure suppression. This air injection may induce a variety of hydrodynamic loads on the suppression pool and its internal structures. In this paper a new multidimensional, finite-difference method, SOLA-VOF, is applied to obtain an understanding of the basic fluid dynamics associated with the vent clearing process. Calculations are presented and compared with data obtained in two small scale laboratory test programs designed to model aspects of the G. E. MARK I and MARK II pressure suppression systems.

Load history variations associated with containers having movable bottom walls are investigated and compared. It is found that significant pressure variations are associated with relatively small container deformation. In the 1/12 apparatus, for instance, a 0.48 mm vertical displacement of the 28 cm diameter pool is sufficient to produce approximately an 11.2% variation in absolute peak pressure on the pool floor.

In some cases these modified peak loads are computed to be larger, rather than smaller, in deformable or movable containers. This happens when walls rebound and contribute a local pressure increase. Such increases do not signify a potentially more damaging load, but do emphasize the care that must be exercised in designing and interpreting data obtained in experimental facilities.

Peak loads are also found to depend on geometric variations of the vent-pool system. For example, in some cases maximum down loads are determined by the driving air pressure and the hydrostatic water head, while in other cases there may be significant water acceleration (dynamic) effects.

The current practice of operating some BWR plants with a small positive pressure differential between the containment and suppression pool compartments has also been studied computationally. A positive pressure differential means that a lower water level initially exists in the vents relative to the suppression pool surface. Calculated results reveal how this practice affects the different hydrodynamic load mechanisms. In particular, peak down loads can be significantly reduced by this practice if it results in vent clearing before the reactor containment pressure has reached its asymptotic level. However, when a constant containment pressure is used, as in some laboratory experiments, peak down loads are not significantly influenced by the initial level of water in the vents.

I. Introduction

In a postulated loss-of-coolant accident (LOCA) in a boiling water reactor (BWR), air is initially forced through vent pipes into large water pools designed for steam pressure suppression. This air injection may induce a variety of hydrodynamic loads on the suppression pool and its internal structures. In this paper a relatively new multidimensional, finite- difference method [1], SOLA-VOF, is described and applied to a variety of studies associated with vent clearing processes.

The basic calculational technique is briefly outlined in the next section. Then, in Sec. III, the code is illustrated through application to two single vent scale models that have been used for extensive experimental studies [2,3]. Pressure histories on the floor and ceiling of the pool container are used as a measure of the hydrodynamic loading experienced by the suppression pool. The SOLA-VOF calculations clearly show how these pressures are altered when the pool is allowed to move, when air bubbles are present in the water, and when certain changes are made in the geometry and initial conditions.

II. Outline of the Computational Method

The SOLA-VOF code provides a numerical solution algorithm for the time-dependent two-dimensional Navier-Stokes equations. Finite-difference approximations are used with respect to a fixed mesh of computational cells. Although basically designed for incompressible fluid dynamics, the code can treat compressibility effects [4] provided density variations are not excessive (say, less than 10%). The general solution method is the same as that used in other codes in the SOLA series [5]. However, SOLA-VOF also possesses several novel features that make it particularly well-suited to the type of hydrodynamic flows generated in BWR suppression pools. Most noteworthy is its ability to treat arbitrary free-surface configurations in a logically simple way. It can simultaneously treat any number of disconnected free surfaces, and automatically handles surfaces that are computed to coalesce or break apart. For example, no special logic is required when the air bubble generated at the end of the submerged vent breaks through the top pool surface. To accomplish this generality, SOLA-VOF employs a function representing the local fluid volume fraction. Within the fluid this function has a value of unity, while in void regions its value is zero. A free surface is defined at locations where the function has a value of 1/2. Derivatives of the function are used to define normal directions to the free surfaces. Knowing these normal directions and function magnitudes in the finite-difference mesh allows us to easily reconstruct fluid interfaces for the application of free surface boundary conditions.

To make this method work, special care must be taken in the manner in which the kinematic equation describing the evolution of the volume function is numerically approximated. SOLA-VOF uses a Donor-Acceptor convective flux approximation [6] that keeps interfaces sharply defined.

In addition, SOLA-VOF uses a mesh of variable rectangular cells, which provides some flexibility to increase local spatial resolution without the need for an excessively large mesh. Because it also has a compressible fluid capability, it could be used to investigate the consequences of steam bubble collapse, chugging, or other phenomena involving high frequency pressure pulses.

Further code details and illustrations of SOLA-VOF can be found in Refs. [7-9].

III. Applications to Vent Clearing Phenomena

There have been several experimental programs conducted using single vent geometries to gain an understanding of vent clearing hydrodynamics. SOLA-VOF has been used to computationally duplicate two of these studies [7-8]. One is the scaling study performed at MIT in Massachusetts, which used a single axisymmetric vent in a cylindrical vessel [2]. The MIT device was roughly a 1/12 model of a G. E. MARK I suppression pool; it was not strictly a scaled model. The other study was conducted by SRI International in California, using a 1/13.3 scaled model of a G. E. MARK II pressure suppression system [3]. The relative sizes and shapes of these experimental devices are shown in Fig. 1. It should be noted that the SRI tests used a taller vessel and a deeper vent submergence. The SRI tests were also performed using a ramped driving pressure in the dry well, while the MIT tests employed a constant driving pressure. As we shall see, these differences do lead to some qualitative differences in the hydrodynamic loading histories.

3.1 A Sample Vent Clearing Calculation

Figure 2 shows typical velocity and fluid configuration results obtained in a calculation designed to simulate an MIT test using a 28 cm diameter vessel. A typical computed floor pressure history is shown in Fig. 3 in comparison with the corresponding experimental results. In this example the experimentally measured floor pressure has a small second peak following the large first peak that occurs shortly after the vent pipe has cleared of water. In some tests more secondary oscillations have been observed, often with relatively low frequencies, like that in Fig. 3, or with much higher frequencies. At least two possible explanations for these oscillations have been suggested: They may be caused by a lack of rigidity in the experimental apparatus [10], or by the presence of air bubbles suspended in the pool water [2]. It seems likely that both effects have been present in many of the tests reported. Calculations with the SOLA-VOF code offer a means of sorting out these effects and independently assessing their consequences as illustrated in the next two sections.

3.2 Influence of Vertical Vessel Motion on Floor Pressure

Let us assume that the model suppression pool is not rigidly tied down, but can execute simple harmonic motion in the vertical direction with period 12.25 ms. Calculations of the coupled fluid-structure system produce the floor pressure history shown in Fig. 4. Here the results are shown in comparison with a calculation assuming a rigidly supported vessel. These results are qualitatively similar to the results obtained in the 1/5 scale MARK I tests conducted at Lawrence Livermore Laboratory [10] and to more recent tests at MIT that used a flexible bottom plate in the vessel [11].

3.3 Influence of Air Bubbles on Floor Pressure

Air bubbles can accumulate in the pool water, for example, by running repeated tests with insufficient time between tests. When this happens the effective compressibility of the water is significantly increased. The consequences of an increased compressibility are obvious from the calculated floor pressures shown in Fig. 5, which are compared to calculational results obtained assuming an incompressible fluid. In this example the sound speed of the air-water mixture was set to approximately 1/10 the speed of sound in pure water.

The observed pressure oscillations in this case are caused by a "bouncing" of the water still resting on the floor. Cases 3.2 and 3.3 show that the introduction of a little softness in either the vessel support or in the pool water leads to higher peak floor pressures. If sufficient softness is introduced into the system one would expect to eventually see a reduction in the peak pressure. In any case, it is clear that experiments used to measure peak loads must be carefully designed and their results carefully interpreted to avoid these kinds of errors.

3.4 Other Influences on Floor Pressure

The geometric differences between the MIT and SRI tests offer an interesting comparison. In the MIT tests and in the SOLA-VOF calculations of these tests it was observed that the first peak in floor pressure was equal to the gas pressure in the vent plus the hydrostatic head of the water still resting on the floor. In the SRI tests this was not the case. Calculations indicate that the peak floor pressure is approximately 9.4% higher than the gas plus hydrostatic pressure because of local fluid accelerations. Apparently the geometric changes associated with a deeper vent submergence and smaller pool to vent area ratio are responsible for this result.

Based on the above observation it should be possible to reduce the peak floor pressure in the SRI apparatus, but not in the MIT apparatus, by lowering the initial level of water in the vent. A lower water level means that vent clearing will occur sooner. Thus, in the SRI case the vent pressure, which contributes most to the peak floor pressure, is less because it occurs earlier in the dry well pressurization history. In the MIT apparatus, however, the dry well is at a constant pressure and an earlier clearing of the vent does not alter the vent pressure at the time of peak floor pressure. These speculations have been verified by SOLA-VOF calculations, which also show that ceiling and wall pressures are likewise reduced by lowering the initial water level in the vent.

Acknowledgment

This work was supported by the Electric Power Research Institute. The authors acknowledge their appreciation to John J. Carey, Project Manager, for his interest and encouragement during the course of this work.

References

[1] Nichols, B. D. and Hirt, C. W., "Methods for Calculating Multi-Dimensional, Transient Free Surface Flows Past Bodies," Proc. of the 1st Intern. Conf. on Numerical Ship Hydrodynamic, Gaithersburg, MD, (Oct. 1975).

[2] Anderson, W. G., Huber, P. W., and Sonin, A. A., "Small Scale Modeling of Hydrodynamic Forces in Pressure Suppression Systems, Final Report," report prepared for the Division of Reactor Safety Research, U. S. Nuclear Regulatory Commission NUREG/CR-003 (1978).

[3] Kiang, R. L. and Jeuck, P. R., "A Study of Pool Swell Dynamics in a Mark II Single-Cell Model," SRI International Report, Oct. 1978 (draft).

[4] Hirt, C. W. and Nichols, B. D., "A Method for Adding Limited Compressibility to Incompressible Hydrocodes," report prepared for Electric Power Research Institute, to be published (1979); Los Alamos Scientific Laboratory Preprint LA-UR-79-375.

[5] Hirt, C. W., Nichols, B. D., and Romero, N. C., "SOLA - A Numerical Solution Algorithm for Transient Fluid Flows," Los Alamos Scientific Laboratory report LA-5852 (1975); Cloutman, L. D., Hirt, C. W., and Romero, N. C., "SOLA-ICE: A Numerical Solution Algorithm for Transient Compressible Fluid Flows," Los Alamos Scientific Laboratory report LA-6236 (1976).

[6] Johnson, W. E., "Development and Application of Computer Programs Related to Hypervelocity Impact," Systems, Science, and Software report 3SR-353 (1970).

[7] Nichols, B. D. and Hirt, C. W., "Numerical Simulation of BWR Vent Clearing Hydrodynamics," ANS 1978 Annual Meeting, San Diego, CA, June 1978; extended manuscript to be published by Electric Power Research Institute (1979).

[8] Hirt, C. W. and Nichols, B. D., "Numerical Simulation of Pool Swell in a Mark II Single-Cell Model," report prepared for Electric Power Research Institute, to be published (1979).

[9] Nichols, B. D. and Hirt, C. W., "SOLA-VOF: A Solution Algorithm for the Dynamics of an Incompressible Fluid Containing Multiple Free Surfaces," Los Alamos Scientific Laboratory report in preparation.

[10] Pitts, J. H. and McCauley, E. W., "Results from the 1/5 - Scale Mark I BWR Pressure Suppression Experiment," presented at the 5th Water Reactor Safety Research Information Meeting, Gaithersburg, MD, Nov. 1977.

[11] Huber, P. W., personal communication (1978).

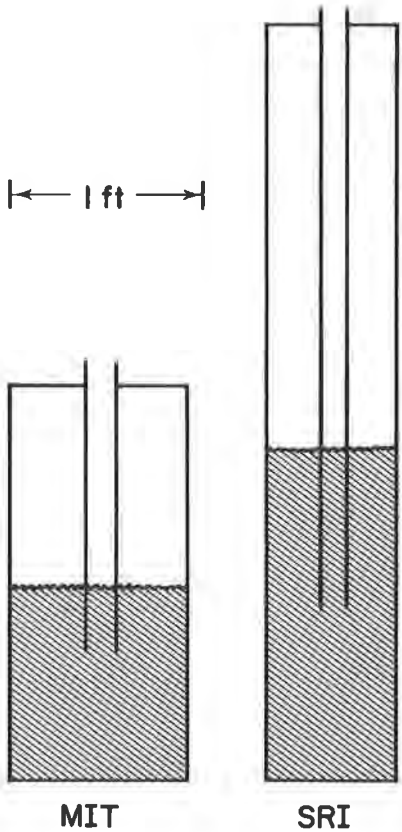

Fig. 1. Schematic comparison of the MIT and SRI test apparatus.

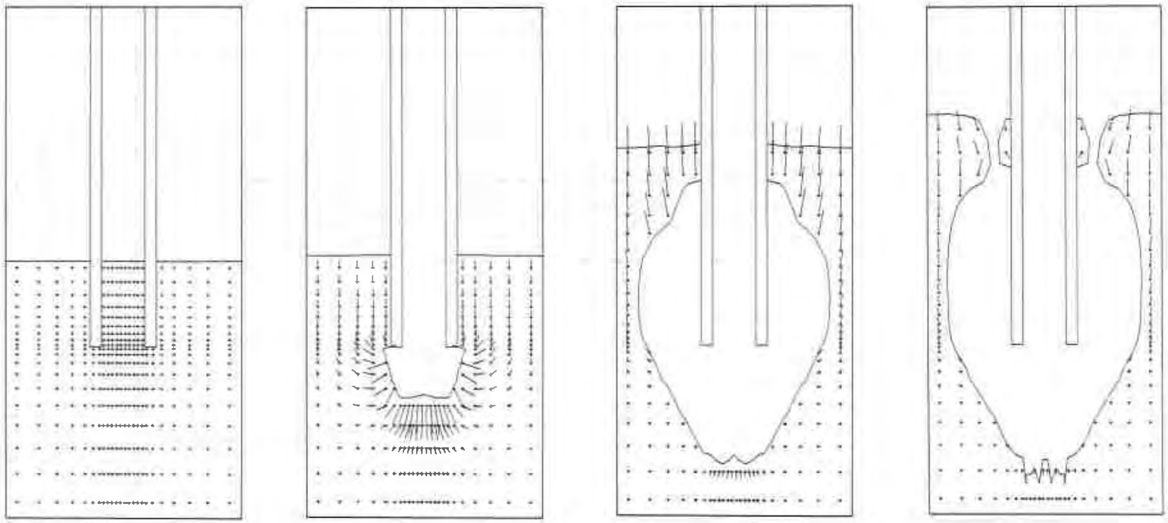

Fig. 2. Typical water configuration and velocity plot computed in a simulation of an MIT test. Times are 0, 40, 77, and 87.5 ms.

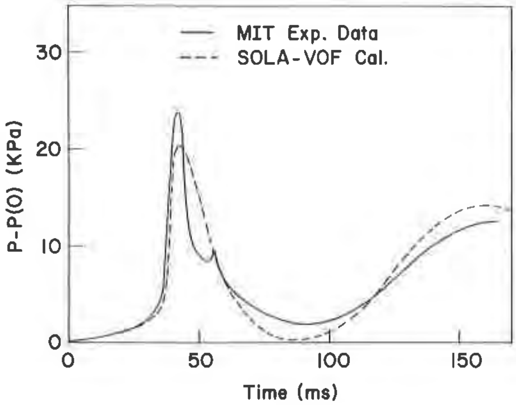

Fig. 3.

Comparison of computed and measured floor pressure histories in MIT apparatus.

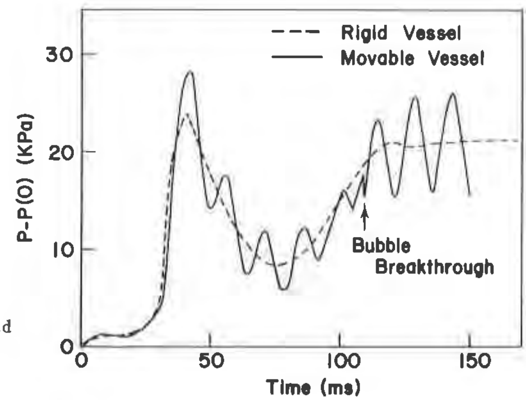

Fig. 4.

Comparison of floor pressure histories computed with and without dynamic response of vessel.

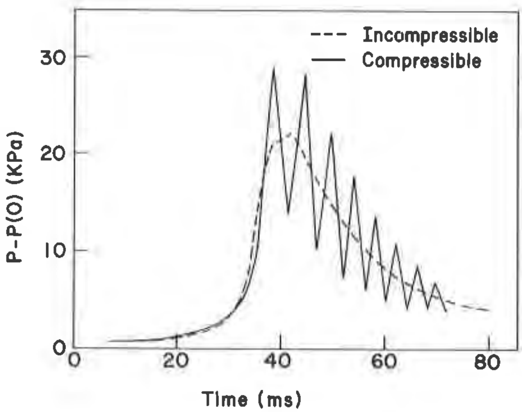

Fig. 5.

Comparison of floor pressure histories computed with and without fluid compressibility.